

MINIATURE INTEGRATED CO-AXIAL CURRENT SHUNT FOR HIGH FREQUENCY SWITCHING POWER ELECTRONICS

A.L.J. Joannou* D.C. Pentz*

* *Group on Electronic Energy Processing (GEEP), Dept. of Electrical and Electronic Engineering Science, Corner of University Road and Kingsway Road, University of Johannesburg, Johannesburg 2006, South Africa E-mail: aljoannou@gmail.com*

Abstract: Power electronic converters are now able to operate at very high frequencies due to the development in GaN and SiC power semi-conductor technologies. Measuring such high frequencies with rise and fall times of a few nanoseconds requires specialised instruments and a good knowledge of measurement techniques. This paper introduces a current shunt designed to be integrated into these high frequency power electronic converters. The shunt is required to have a high bandwidth in order to reduce the measurement error.

Keywords: Current measurement, high frequency, co-axial shunt.

1. INTRODUCTION

The drive towards smaller power electronic converters has forced the operating frequencies of converters to increase, such that the normally large energy storage elements of these converters can be reduced in physical size. Although size limitations still exist due to the magnetic elements, the overall reduction is still considerable. Previously, the limitation of the maximum switching frequency of these converters was the transistors.

Developments in power semi-conductor technology introduced Silicon carbide (SiC) power switching transistors which are able to switch in the RF range, and even newer semi-conductors have been introduced for power switching, the GaN transistors, which are said to be able to achieve even better characteristics than the SiC devices as discussed in [1] and [2]. These recent developments in semi-conductor switches have now left other technologies to trail. One such technology has been identified as accurate current measurement. Although actual measurement probes are well developed, especially for voltage measurement, the high frequency switching operation of the circuit can cause stray flux to couple onto the measurement leads causing considerable measurement error.

Current probes also often require that a loop be added to accommodate a current probe. This loop adds inductance to the circuit which will change the operating characteristics of the circuit. Ideally HF and RF switching power electronic circuits should have as little parasitic inductance and capacitance as possible. This implies that current and voltage sensors should be carefully designed and characterised to ensure that the parasitic impedance they add is negligible, or at least will not drastically affect the circuit operation. This is especially important for new switching devices such as eGaN FETs [3].

2. CURRENT MEASUREMENT IN POWER ELECTRONIC CONVERTERS

Measuring current in power electronic circuits is important for several reasons, such as protection and control. Measuring current in RF devices in the past was not a concern, since the devices were either low power, or operated under sinusoidal conditions. Measuring the pulsed current waveforms in power electronic circuits requires current sensors with high bandwidth capability.

The bandwidth of any device corresponds to the 3dB knee frequency which also correlates to a 45 degree phase shift at that 3dB point. This large phase shift can cause inaccurate measurement and possibly failure in the circuit. For instance, if a phase arm is switching out of phase, a phase shift (which correlates to a time shift) in either of the drive signals can cause a short circuit current through the switches which would be detrimental to the circuit and/or the power switches. This is why it is important to realise that measurement specifications for hard switching power electronic circuits must be strict and that the 3dB rated frequency is not a true or sufficient figure of merit.

Current sensors, specifically in power electronic circuits, aim to achieve the following characteristics as listed in [4]:

- Compact size with a very low profile
- Ease of manufacture and low cost
- High bandwidth for high frequency operation
- Fast response with low parasitic elements introduced
- Reliable with good noise immunity
- High stability with varying temperature

The criteria listed above are used as guidelines while designing the integratable shunt discussed in this paper. The accuracy of a current sensor relies heavily on the impedance matching of the input and outputs of the device under test [5]. Several different shunt technologies are discussed next.

3. INTEGRATED CURRENT MEASUREMENT TECHNIQUES

3.1 Integrated current transformer

Current transformers still require a magnetically permeable core, even at high frequencies. This core can do no less but add to the layout inductance of the power circuit as well as the inherent inductance of the current sensor which limits its rise time response [6]. Another problem with current transformer sensing methods is that only AC waveforms can be measured.

3.2 Current sensing on chip

Some designers have even tested the idea of integrating the sensing technology on the chip for applications as in [5] and [7]. The advantage of current sensing on chip is that the inherent inductance of the sensor is small. Even so, physically measuring this current can still introduce measurement error. This is costly and is not available for all power switches since it is part of the chip manufacturing.

The on state resistance can also be used to measure the current. As more current passes through the power switch, the on state resistance varies as a function of temperature, thus varying the measured quantities. The true limitation of current sensing on chip is the temperature distribution in the chip.

3.3 Integrated Rogowski coil

Rogowski coils can be integrated into a circuit. The limitation of the Rogowski current sensor is the integrator, since the coil itself can be designed to have a high bandwidth [6]. In order to achieve a high bandwidth device, the cost of the integrator exponentially increases making this an unfeasible option.

3.4 GMI and GMR current sensing

Giant Magneto Impedance (GMI) sensors and Giant Magneto Resistive (GMR) sensors [6] are sensor technologies which can also be integrated into the power electronic circuit. This is because their method of operation allows for these devices to reduce in size significantly as discussed in [8]. Although these GMI and GMR devices can be made relatively small, they are costly and complex to be designed into a common power electronic circuit, as well as susceptible to the EMI generated by the power electronics.

3.5 Integrated planar shunt

This shunt resistor is constructed using thick film metallisation technology [6]. The advantage of this shunt design is its ultra-low profile and low cost. The resistance may vary due to the contact resistance [4].

3.6 Co-axial shunt resistor

A typical co-axial shunt resistor is shown in Figure 1. The idea behind the co-axial shunt resistor is to create a shunt with low inherent parasitic elements, high bandwidth and also to be able to measure with low measurement noise. This is achieved by physically placing the measurement lead wire within the field free region of the shunt resistor. The region is field free because it is inside the current carrying tube conductor as indicated in Figure 1, and can be explained with Amperes circuital law. This law states that the magnetic field enclosed by any enclosed path is equal to the current enclosed by that path [9]. Hence the enclosed area inside the shunt will have no magnetic field. The common type of co-axial shunt resistors as indicated in Figure 1 is bulky and is physically large so that it can thermally dissipate the losses. The disadvantage of shunt resistors is they do not offer isolation and they are temperature dependent.

Simply miniaturising the shunt will reduce the area from which it can dissipate the thermal energy losses, hence lowering the power capability of the shunt. The shunt needs to be miniaturised so that it can be integrated into the PCB of the power electronic converter and still be able to dissipate the thermal energy.

The shunts that are discussed in this paper are for low or high voltage, but low current applications, namely below 20 amperes. This low current will correspond to the voltage drop across the shunt resistor being comparable with the leakage flux that could induce measurement noise. Thus the shunt needs to be designed such that the desired signal can be differentiated from the measurement error.

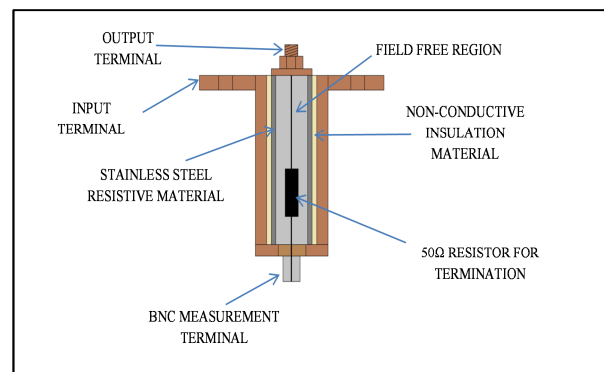


Figure 1: Co-axial shunt resistor

4. MINIATURE INTEGRATED CO-AXIAL SHUNT

Shunt resistors are known to be one of the most accurate and simplest methods of sensing current as discussed in [10]. They are also cost effective. The current is simply determined by the voltage drop across the resistor using Ohm's Law. Therefore it is imperative that the shunts are designed to reduce the effects of parasitic elements. These reasons thus lead to the proposed shunt design

which resembles a co-axial shunt resistor. To reduce the parasitic elements, an integrated design is implemented.

Inspired by the more common co-axial shunt, this shunt resistor mimics the operation to achieve similar characteristics but physically at a much smaller scale. The resistance of the shunt should be small (normally in the order of a few milli-ohm) so that the losses due to the shunt are negligible (1.286 W at 10A). The shunt should also be designed so that the stray flux that could possibly couple onto the measurement is negligible compared to the actual current measurement, hence low measurement error.

The performance of the shunt is dependent on its size as well as placing the measurement leads in a low field region as discussed earlier as well as in [4]. Therefore by miniaturising the design, the shunt resistor should have better high frequency performance. The next issue is the thermal dissipation of the shunt.

In order to keep the cost low, the design should be simple and easy to implement, no exotic metals are used in this miniature shunt design. Instead surface mount (SMD) resistors are used as the resistive material. A cross section of the miniature or even micro shunt design is shown in Figure 2 and Figure 4. The current paths through this shunt are indicated in Figure 4. The current flow in adjacent current carrying paths is in opposite directions, the field around the paths will be weak fields because of the field cancellation. This electromagnetic effect will also cause a high current concentration on the edges of the conductors facing each other on the adjacent paths.

Skin depth and proximity effects are critical phenomena which can affect the resistance and inductance of the shunt. The current distribution of the shunt must be balanced to ensure even current flow throughout the shunt. The arrangement of the SMD resistors is indicated in Figure 3. This concentric arrangement of the SMD resistors of equal resistance will ensure a relatively even current distribution at high frequencies. This also allows for even heat dissipation of the SMD resistors. In Figure 3, eight resistors (the shunt design can include more resistors to design as discussed later) are shown connected in parallel. Connecting the resistors in parallel will increase the electrical power capability of the shunt. Although from a thermal perspective, this implies that the heat dissipating surfaces are closer together. Also, the resistors power dissipation specifications are tested in free air and not when packed closely together.

This shunt design is cost effective and easy to implement and integrate into any high frequency circuit design. This type of shunt can be used for feedback control in the converter, but it is suggested measurement terminals are reconsidered. The components used for this shunt are also chosen as common components which are often used in high frequency power electronic converters. The

constructed integrated co-axial shunt resistor is shown in Figure 5.

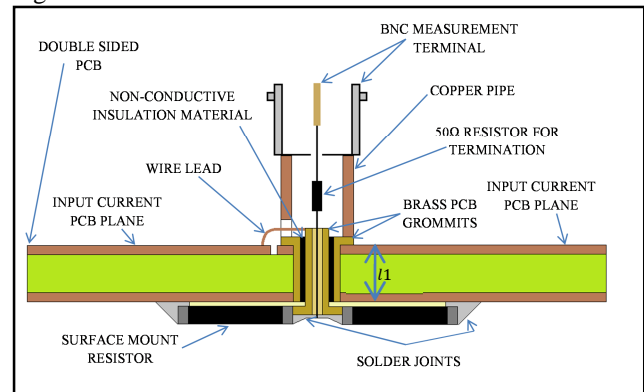


Figure 2: Cross section of miniature integrated co-axial shunt resistor

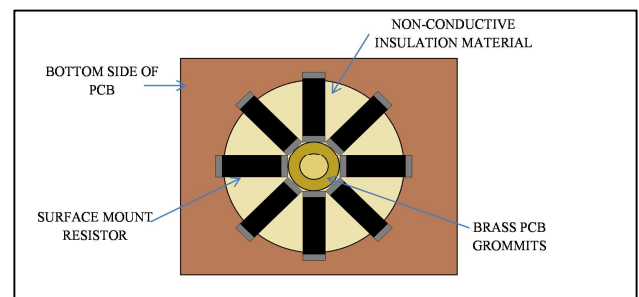


Figure 3: Bottom view of miniature shunt indicating concentric arrangement of SMD resistors

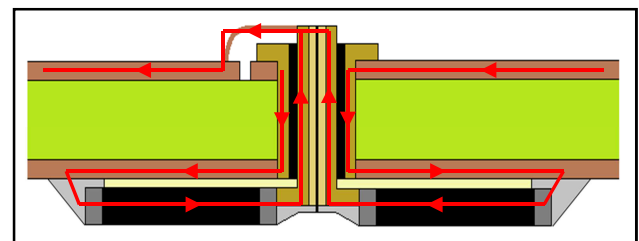


Figure 4: Current path of shunt resistor indicating currents in adjacent paths flowing in opposite directions

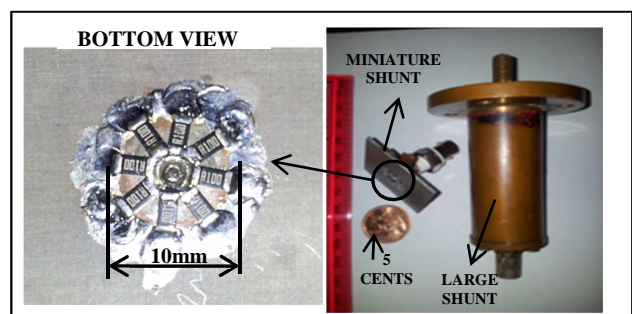


Figure 5: Photo of actual shunt resistor

5. MINIATURE INTEGRATED CO-AXIAL SHUNT DESIGN PROCEDURE

The general approach to design such a shunt is explained below. This is the procedure that was followed during the design of the shunt discussed in this paper.

1. Choose maximum current to flow through the shunt, I [A].
2. Choose the maximum power dissipation of the shunt, P [W].
3. Determine the resistance of the shunt, $R = \frac{P}{I^2}$
4. Determine if the voltage drop measured across the shunt will be sufficient $V = IR$. If not, then revisit steps 1 to 3.
5. Using both the resistance of the shunt as well as the power rating, choose the number of resistors to be placed in parallel. Note that all resistors should be the same value to ensure even current and power distribution. Also, the size of the shunt should be realised. Using too many resistors in parallel becomes impractical. In this step one should also consider the size of the grommet/via that will be used. Ideally the resistors should all be spaced equally around the shunt.

Specifically for the shunt discussed in this paper, the maximum current to be measured is $I=12A$. The maximum power dissipation is chosen as $2W$. Thus the resistance is initially chosen as $R=0.0125\Omega$. Therefore at $12A$, the voltage drop across the shunt will be $150mV$ which is sufficient. Next the resistors were chosen to be $0.25W$ per 1206 SMD package. This means that the number of required resistors would be

$$No. \text{ resistors} = \frac{\text{Total power}}{\text{Power per package}} = \frac{2}{0.25} = 8 \quad (1)$$

The most readily available resistance value is 0.1Ω for which a parallel combination of 8 resistors result in a resistance of 0.0125Ω as required. SMD resistors are chosen because of their size advantage but also because they are flat and can be placed relatively close to the PCB, which will result in a lower inherent inductance. Obviously the more resistors, the better, since the surface covered would be larger with closer resemblance to a solid disc. A solid disc will have better current distribution than the discrete resistors. A solid resistive disc can be made using embedded resistor printed circuit board as found in [11]. Such PCB is not readily available and the resistive material used may vary in resistance.

6. CHARACTERISATION

Characterising the shunt resistor so that the results are in fact meaningful is possibly the most important aspect. The impedance measurement guidelines can be followed in [12], [13] and [14].

6.1 DC characterization

Two tests were performed under DC conditions. One test is to determine the DC resistance, and the other to determine the rated thermal capacity versus the experimental thermal capacity at the specified current of $12A$. A four point wire measurement using a FLUKE 5520A Calibrator was used to measure the DC resistance

of the miniature co-axial shunt resistor. The resistance was measured to be $12.86m\Omega$. The theoretical resistance is effectively eight 0.1Ω resistors in parallel which is equal to $12.5m\Omega$. Thus the measured resistance is slightly higher which is acceptable and highly likely due to the tolerance ratings of the resistors, solder as well as contact resistance which is added.

Each resistor used is characterised to have a thermal power dissipation of $0.25W$ in free air. The resistors are placed in close proximity to each other. This yields a problem since the thermal dissipating areas are now close to each other. This will de-rate power specification of each resistor package. Although it is assumed that the maximum possible rating is the listed rating for free air. Since eight 0.25 watt resistors were used, the total thermal dissipation is 2 watts. The DC resistance is $12.86m\Omega$, thus the theoretical power loss at $12A$ is

$$P = I^2 R = (12)^2 (12.86 \times 10^{-3}) = 1.85 W \quad (2)$$

Theoretically, the shunt should be able to dissipate the thermal losses. A continuous supply of $12A$ DC was passed through the miniature shunt to test its thermal capability. The shunt was tested for one hour without any sign of failure of the shunt, but a slight increase in resistance because of the rise in temperature, which is as expected.

6.2 Frequency characterisation

The shunts' frequency characteristics were measured using two different methods.

Impedance analyser results:

An Agilent 4294A impedance analyser was first used to characterise the shunt resistor. The miniature shunt was measured against a regular large size co-axial shunt, both with the same measurement procedure and setup. The leads of the shunts were initially calibrated out of the measurement, so that only the shunt impedance could be measured.

At low impedances, the Agilent 4294A loses much of its accuracy. Therefore these results are not much of an indication of the characteristics of the shunt. These results are shown in Figure 6 and Figure 7. Figure 6 indicates that the miniature shunt resistor has a 45 degree phase shift at $1.2MHz$, which is questionable. To obtain a reference to this result, a regular large size co-axial shunt resistor was also measured using the same device and the results are indicated in Figure 7. The regular co-axial shunt resistor measures a 45 degree phase shift at just over 300 kHz. This is highly unlikely which leads one to believe that these results are questionable. This could be due to the fact that the impedance analyser used is incapable of measuring accurately at such low impedances. Another experimental characterisation setup is required to justify these results.

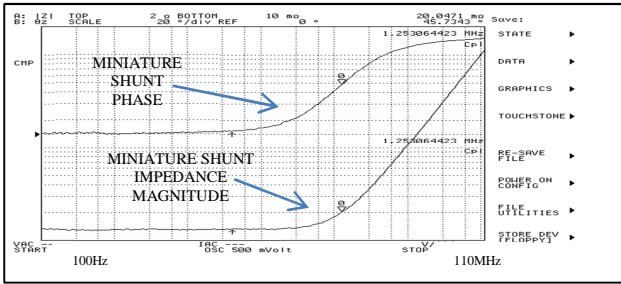


Figure 6: Impedance and phase bode plots captures for miniature shunt resistor

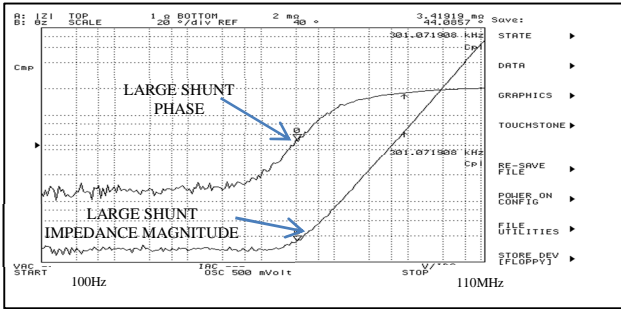


Figure 7: Impedance and phase bode plots captures for regular large co-axial shunt resistor

Vector network analyser results:

An Agilent 8712B Vector network analyser was used to obtain a through-transfer function of the mini shunt. The same procedure was used for the common shunt. Again it should be noted that this instrument also loses accuracy at such low impedances. These results indicate a dominant resonant point at 807MHz, which can be seen in Figure 8. This plot indicates that the miniature shunt is in fact inductive before 807MHz. This needs to be verified with an alternative measurement technique.

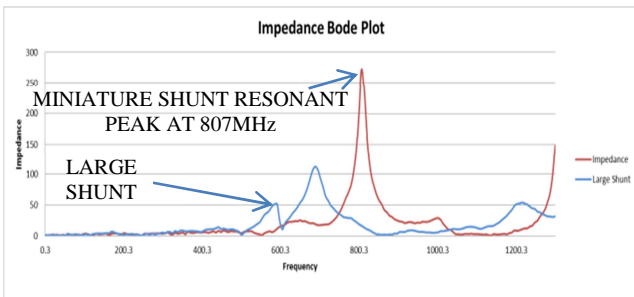


Figure 8: Impedance bode plot for miniature and large co-axial shunt resistor

6.3 Step- response results

An EPC 9001 development board was used which implements eGaN FETs as the power switching semiconductors. These eGaN FETs are able to switch within a few nanoseconds. The shunt resistor was then placed in series with a constructed low inductance resistive load. This load was constructed such that there is uniform current distribution through the load while still maintaining a low inductance. The experimental setup, including the low inductance load is indicated in Figure

9. The experiment was performed at 10 watts, (10V @ 1A).

The power circuit was then setup to induce a 1A current step of a few nanoseconds rise time. The current through the resistor load and shunt was then measured using the shunt resistor and a Tektronix TCP0030 120MHz current probe. The voltage across the resistor load was measured using a Tektronix P5050 voltage probe and a DPO7254 Tektronix oscilloscope was used. These results are indicated in Figure 10.

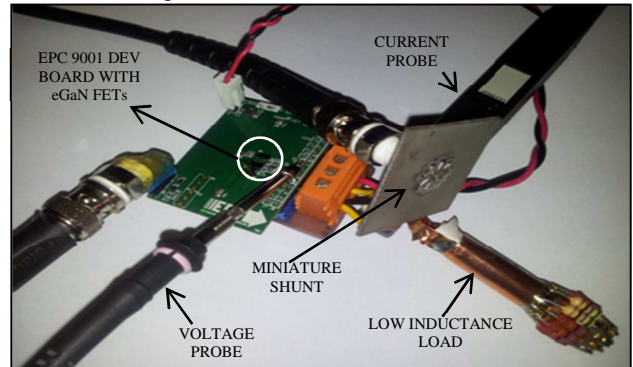


Figure 9: Experimental setup

Figure 10 indicates that there are oscillations in the voltage waveform. This could be due to the complex nature of the load (inherent inductance and capacitance) as well as the inductive loop of the ground return path of the voltage probe, even though the ground loop wire of the voltage probe was removed and short connection loops were soldered in an effort to reduce the voltage probe return loop.

There is also a noticeable delay in the response time of the current probe to the voltage. This could be due to the delay of the hall sensor, long co-axial cable length and amplifier setup of the current probe. The oscillations in the response waveform of the shunt resistor indicated in Figure 10 could be due to reflections and unbalanced source impedance matching and inherent inductance and capacitance resonance of the shunt. This can cause the shunt response to rise faster than the actual measurement. It was also observed that there was no noticeable difference in the shunt measurement with the current probe in the circuit or not.

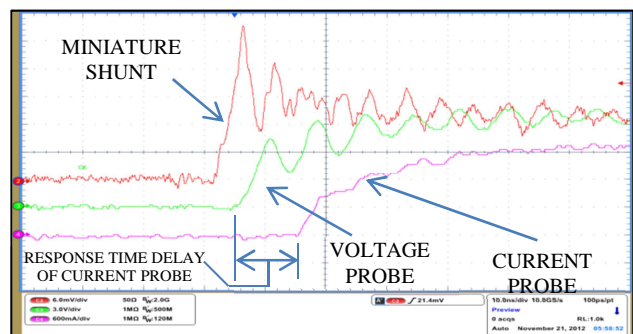


Figure 10: Step response of miniature shunt resistor and current probe

Using the rise time response of the miniature shunt, the bandwidth of the shunt can be estimated using the following equation from [15].

$$t_r = \frac{0.338}{f_{3dB}} \quad (3)$$

The rise time of the shunt to the step response is measured using the oscilloscope to be 2.35ns. This corresponds to a bandwidth of $f_{3dB} = 143\text{MHz}$.

7. FUTURE WORK

The results are not yet satisfactory due to the uncertainty of the results and therefore require more work. Alternative methods of characterising the miniature shunt resistor are being investigated to verify the results presented in this paper. The large shunt still needs to be placed in the same experimental setup to observe its response under the same conditions and compared to the results of the miniature shunt.

The miniature integrated shunt has also been simulated in COMSOL 4.3a. The electromagnetic simulation results are being analysed. The simulated thermal aspects are still to be investigated. The equivalent circuit and theoretical inherent parasitic elements of the miniature co-axial shunt are also being addressed. The equivalent-circuit impedance can also be used to verify the measured characteristics. Implementing the miniature integrated shunt into a HF and possibly RF hard switching power electronic converter circuit using GaN power transistors is also being looked into. The possibility of using embedded thin film resistor PCB and integrating the shunt into such PCB material will allow for better electromagnetic characteristics. This will be investigated and implemented in the near future.

8. CONCLUSION

A current sensor for integrated HF current measurements has been discussed in this paper. The shunt design is low cost and easy to integrate into HF power electronic circuits. The estimated bandwidth of the shunt is 143MHz matches expensive current sensor technologies, such as current probes. The bandwidth also indicates that this type of integrated shunt is capable of measuring rise and fall times of a few nanoseconds. This is suitable for the rated switching times of GaN power transistors. Although this shunt design is intended for integration for GaN based power electronic circuits, it can be integrated into any circuit in which a non-isolated current sensor is required.

9. ACKNOWLEDGEMENTS

I would like to thank Prof. J Daan van Wyk for the original idea on the shunt and suggested experiments. I would also like to thank Dr. Arnold de Beer from the University of Johannesburg and Prof. Ivan Hofsafer from

the University of Witwatersrand for their assistance in measurement with the network and impedance analysers.

10. REFERENCES

- [1] A Lidow, "Is it the end of the road for silicon in power conversion?," in *CIPS*, Nuremburg, 2010.
- [2] N Kaminski and O Hilt, "SiC and GaN devices-competition or coexistence?," in *CIPS*, Nuremburg, 2012.
- [3] A Lidow. (2011) EPC Efficient Power Conversion. [Online]. <http://www.epc-co.com>
- [4] J A Ferreira, W A Cronje, and W A Relihan, "Integration of high frequency current shunts in power electronic circuits," in *IEEE Power electronics specialists conference (PESC)*, Toledo, Spain, 1992, pp. 1284-1290.
- [5] YC Huang, HH Hsieh, and LH Lu, "A low noise amplifier with integrated current and power sensors for RF and BIST applications," in *IEEE-VLSI Test Symposium*, 2007, pp. 401-408.
- [6] C Xiao, L Zhao, T Asada, W G Odendaal, and J D van Wyk, "An overview of integratable current sensor technologies," *IEEE-IAS*, 2003.
- [7] KH Cheng, CW Su, and HH Ko, "A high-accuracy and high-efficiency on-chip current sensing for current mode control CMOS DC-DC buck converter," in *IEEE-Electronics circuits and systems (ICECS)*, 2008, pp. 458-461.
- [8] E R Olson and R D Lorenz, "Integrating giant magnetoresistive current and thermal sensors in power electronic modules," in *IEEE-Applied power electronics conference and exposition (APEC)*, 2003, pp. 773-777.
- [9] W H Hayt and J A Buck, *Engineering electromagnetics*, 7th ed. New York, United States: McGraw Hill Publishers, 2006.
- [10] W Pfeiffer, "Ultra-high speed methods of measurement for the investigation of breakdown development in gasses," *IEEE transactions on instrumentation and emasurement*, vol. IM-26, no. 4, pp. 367-372, December 1977.
- [11] J Wang and S Clouser. Gould Electronics. [Online]. http://www.gould.com/e4/e139/e197/tpyea_r203/tpdownload227/01_ThinFilm_eng.pdf
- [12] Agilent Technologies, 8 Hints for succesful impedance measurements, Application Note 346-4.
- [13] Agilent Technologies, Impedance and network analysis application list, 2012, Revision-2.00.
- [14] Agilent Technologies, Advanced impedance measurement capability of the RF I-V method compared to the network analysis method, Application Note 1369-2.
- [15] H Johnson and M Graham, *High-speed digital design a handbook of black magic*. New Jersey, United states of america: Prentice Hall, 1993.